buildings

Article

Examination of Mixing Proportion in Self-Compacting Gangue-Based Pavement Concrete

Lianjun Chen [1,2], Nan Guo [3], Guoming Liu [1,2,*], Xiaohan Guo [1], Jipeng Zhao [3] and Zhaoxia Liu [2,3,*]

[1] College of Safety and Environmental Engineering, Shandong University of Science and Technology, Qingdao 266590, China; skyskjxz@163.com (L.C.); gxh006788@163.com (X.G.)
[2] State Key Laboratory of Mining Disaster Prevention and Control Co-Founded by Shandong Province and Ministry of Science and Technology, Shandong University of Science and Technology, Qingdao 266590, China
[3] Collage of Energy and Mining Engineering, Shandong University of Science and Technology, Qingdao 266590, China; gnn34031928@163.com (N.G.); jipengzhao0429@163.com (J.Z.)
* Correspondence: skd995978@sdust.edu.cn (G.L.); zhaoxialiu@163.com (Z.L.)

Abstract: In recent years, with the rapid development of the coal-mining industry, the output of gangue has increased at a faster pace, while its utilization remains relatively low. The accumulation of a large amount of gangue has brought about a large environmental problem. In order to improve the utilization rate of waste gangue, and to solve the secondary environmental problems caused by gangue pollution, this paper conducted research on an economic and environmentally friendly gangue-based self-compacting concrete. This study designed aggregate industrial-analysis experiments to analyze the moisture content of the gangue and limestone, finding that the moisture content of gangue is 39% higher than that of limestone. By orthogonal experimental methods, the study investigated the fluidity, compressive strength, splitting strength and abrasion resistance of self-compacting gangue concrete. It was concluded that the optimal replacement rate of gangue for coarse aggregate is around 30%, the optimal replacement rate of fly ash for cement is around 30%, the optimal addition of polycarboxylate superplasticizer is 0.5% of the mass of cementitious materials, and the optimal rate of shear steel fibers is around 1% of the concrete capacity. In addition, this paper investigated the interfacial transition zone (ITZ) of the aggregate–cement slurry and found that the ITZ of gangue aggregate and cement mortar is more likely to generate AFT crystals, which will contribute more to the improvement of the strength of concrete in the early stage. In addition, a field-effect analysis was carried out in this study, and it found that gangue-based self-compacting concrete, as an environmentally friendly material, can basically meet the design requirements of C30 paving concrete.

Keywords: self-compacting concrete; gangue; mixing ratio; interface transition zone (ITZ)

Citation: Chen, L.; Guo, N.; Liu, G.; Guo, X.; Zhao, J.; Liu, Z. Examination of Mixing Proportion in Self-Compacting Gangue-Based Pavement Concrete. *Buildings* **2022**, *12*, 591. https://doi.org/10.3390/buildings12050591

Academic Editor: Elena Ferretti

Received: 3 March 2022
Accepted: 29 April 2022
Published: 2 May 2022

1. Introduction

Solid-waste management has long been a key global concern. On 6 September 2015, the United Nations Environment Programme (UNEP) and the International Solid Waste Association (ISWA) released a report entitled Global Waste Management Outlook, calling on countries to take immediate action to maximize the recycling of resources. On 18 March 2021, China issued the "Guidance on the Comprehensive Utilisation of Bulk Solid Waste in the 14th Five-Year Plan", which states that the comprehensive utilization rate of bulk solid waste such as coal gangue and fly ash should reach 60% [1,2]. Coal, with reserves of over 10 trillion tons, is by far the most used fossil resource in the world. Gangue is the solid waste produced in coal mining. According to incomplete statistics, as of 2021, the accumulated amount of gangue in China has exceeded 6 billion tons, and the number of formatted gangue mountains is 1500 to 1700, covering an area of more than 133 square kilometers. Because of the presence of flammable Fe_2S material in the gangue, which is easy to burn and explode, a large amount of gangue accumulation has had extremely adverse effects on the environment [3,4]. To achieve global sustainable development, the use of gangue is one of the important research topics among scholars from various countries. In recent years, a large number of studies were conducted on the use of gangue ranging from gangue power generation, gangue paving, using gangue as construction materials or chemical raw materials, etc. The results have shown that the compressive strength of gangue concrete could meet the design requirements of C30 concrete and is suitable for low- and medium-strength concrete. Moghadam. et al. [5] summarized the application of gangue as alkali-active material, and found that gangue is rich in silica, alumina and other components that accelerate the hydration of cement to produce AFT, which proves that gangue can be used as an alkaline excitation material of cement. Ashfaq. et al. [6,7] studied the application value of gangue, and found that it can reduce CO_2 emission caused by the procurement and transportation of natural aggregates in the field of geotechnical engineering, which is beneficial to environmental protection. Mei et al. [8] found that there are significant differences in the transition zone of the concrete interface after adding gangue and gravel. With the increase in gangue content, the transition zone of the concrete interface becomes thinner and denser. Meng et al. [9] added gangue as coarse and fine aggregates into concrete and found that the sand ratio was positively correlated with the concrete density and negatively correlated with the porosity within a certain range. The main influencing factor of compressive strength was the particle size of the coarse aggregate, and the compressive strength increased with the increase in particle size. Su et al. [10] found that the compression and anti-splitting failure mode of gangue concrete is mainly gangue fracture, but the water-absorption rate of gangue is higher than that of natural gravel; with the increase in the gangue replacement rate, the water–cement ratio decreased, which is more conducive to the improvement of the concrete compressive strength. Bai et al. [11] found that the stress–strain curve of gangue concrete is similar to that of ordinary concrete in the rising stage. The fitting effect is good, but there is a sudden drop, and the fitting result is discrete from the actual situation.

Self-compacting concrete (SCC) is a kind of concrete that can be completely filled with formwork by gravity alone, without the need for vibratory compaction. Its high flow and filling capacity is what gives it an advantage over ordinary concrete. Self-compacting concrete has high fluidity, high cohesion, high water retention, good durability, and is widely used for filling complex terrain structures and paving [12,13]. Choudhary et al. [14] found that the lower the Ca/Si in the concrete mix, the higher the compressive strength, according to energy spectroscopy. Han et al. [15] found that excessive superplasticizer and vibration will reduce the anti-segregation performance of SCC, and the effect of vibration is more obvious. Xie et al. [16] found that slump flow decreased with increasing coarse-to-fine-aggregate-volume ratio, and the increased coarse-aggregate size also reduced the slump expansion of concrete. Zhu et al. [17] found that the volume ratio of coarse aggregate is negatively correlated with the workability of SCC. When the volume ratio of coarse aggregate is 33% and the grading is (5–10 mm: 10–16 mm: 16–20 mm = 30%: 30%: 40%), the concrete performance is the best. Shi et al. [18] found that fly ash is one of the important additives in SCC. When the amount of fly ash is less than 40% of the total cementitious materials, the fluidity of the concrete is positively correlated with the amount of fly ash. Qiu et al. [19,20] found that the 30% fly-ash content changed the physical and chemical properties of the gangue aggregate interface, reducing the width of both ITZ pores and cracks, and could block the large pores on surface of gangue, reduce its water absorption, fully hydrate the cement, and enhance the interfacial adhesion, so as to improve the mechanical properties of concrete. Amounts of 10% and 40% fly ash will cause large pores in the ITZ. Shcherban et al. [21] studied the effect of micro-silica on the performance of light fiber concrete, and found that when its content is 10% cement, the concrete can have a more dense C-S-H microstructure and improve the mechanical properties.

Steel-fiber concrete is widely used because of its higher compressive strength, splitting strength and flexural strength than normal concrete. Rao, Ghasemi et al. [22,23] found that when the volume fraction of steel fibers is 1.0% and the aspect ratio is 25, SCC has the best performance. The addition of steel fibers causes concrete interface damage to develop from the loading end to the free end. When steel fibers are in the stress-concentration zone and the maximum aggregate particle size is 12.5 mm, the fracture-energy-absorption capacity of concrete can be improved, thereby delaying the damage development of concrete. Ding, Wang et al. [24,25] found that the slump expansion and segregation rate of self-compacting steel-fiber-reinforced concrete are negatively correlated with the fiber coefficient. The segregation phenomenon occurs when the concrete segregation rate exceeds 20%, and the appearance of the concrete surface is affected by excessive cohesion if it is less than 5%. Horňákováet al. [26] studied the effect of steel fibers on ceramic-waste lightweight aggregate concrete and found that the compressive strength of the concrete was not proportional to the amount of steel fibers, even lower than that of the control group. For the splitting strength, it showed a certain promotion effect.

Various scholars have conducted much research on self-compacting concrete, gangue concrete and steel-fiber concrete, but few of them have performed an analysis on combining materials together, and no corresponding proportioning scheme has been made. This study designs a self-compacting gangue-based concrete by the effective combination of the high-flow filling capacity of self-compacting concrete as well as the advantages of gangue concrete and steel-fiber concrete. It is of great significance for improving the utilization rate of industrial-waste gangue, reducing the environmental damage brought about by gangue accumulation, and achieving its engineering value. To this end, this study designed gangue and limestone industrial-analysis experiments and clarified the gangue and limestone in the water-absorption rate, and other aspects of the difference. It used orthogonal experiments as the method to design a ratio experiment for gangue-based self-compacting concrete, and studied the slump expansion, mechanical properties and abrasion resistance of gangue-based self-compacting concrete. It also investigated the gangue aggregate–slurry interface transition zone (ITZ), and established the link between the strength of gangue, the ITZ, and the mechanical properties of concrete. As this study was suitable for use in normal concrete pavements and did not involve aggressive, high CO_2 concentration and water-rich environments, durability testing was not required.

2. Materials and Experiments

2.1. Materials

The study adopted the standard PO. 42. 5 ordinary silicate cement and the fly ash of Grade I. The properties of the cement and fly ash are shown in Table 1.

Table 1. Main chemical composition and content of cement and fly ash /%.

Raw Materials	SiO_2	Al_2O_3	Fe_2O_3	CaO	MgO	K_20	Na_2O	TiO_2	SO_3
OPC	20.43	3.99	4.53	62.37	2.23	1.11	0.19	0.37	4.28
FA	56.24	29.81	5.15	3.12	0.74	1.37	0.41	1.72	0.56

Standard river sand was adopted as the fine aggregate, and its grade is shown in Figure 1, with a fineness modulus of 2.3–3.0 and the parameters are shown in Table 2.

Table 2. Physical parameters of fine aggregate.

Raw Materials	Apparent Density (kg/m^3)	Bulk Density (kg/m^3)	Sediment Percentage (%)	Cl^- Content (%)
Fine aggregeat	2600	1400	2.5	$\leq$0.02

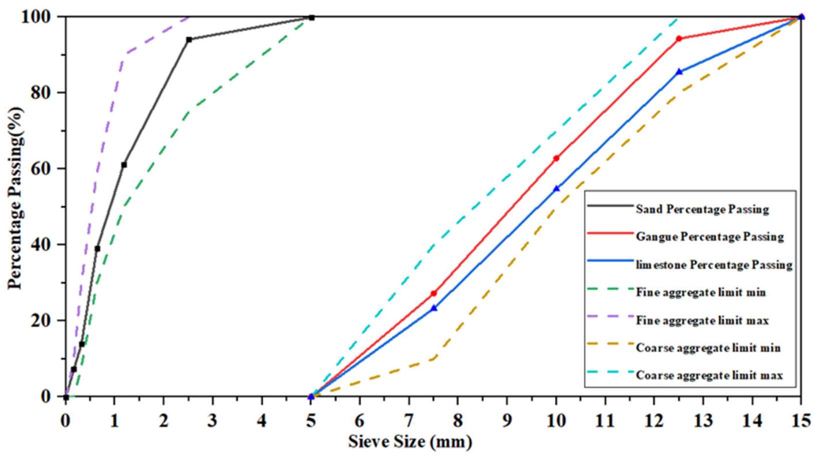

Figure 1. Aggregate grading curve.

According to JGJ/T283-2012 Self-compacting Concrete Application Technical Regulations, the maximum particle size of coarse aggregate should be ≤16 mm. The coarse aggregate used in this study was partly limestone, the average particle size of which was 5 mm–15 mm, the parameters shown in Table 3, and partly non-spontaneous combustion sandstone gangue produced in a mine in Shanxi province, China. The results of gangue specimens in the XRD scanning analysis are shown in Figure 2 and Table 4. The "-" in Table 4 means below the detection limit content. Before use, the gangue was first crushed, which was carried out by an EP-2 jaw crusher to produce the particle size of 3–15 mm. Then the crushed gangue was screened by a new standard square-hole gravel sieve with nominal diameters of 5 mm, 7.5 mm, 12.5 mm and 15 mm. Gangue with a 5–15 mm particle size was selected and screened as shown in Figure 3. The aggregate grading curve is shown in Figure 1. The steel fiber was a shear steel fiber with a length of 25 mm and an equivalent diameter of 0.650 mm. The water-reducing agent was made of polycarboxylic-acid superplasticizer, and the water-reducing rate was 25%.

Table 3. Physical parameters of gravel.

Strength/MPa	Apparent Density (kg/m^3)	Total Content of Needle and Flake Particles (%)	Crushing Indicators (%)	Water Absorption (%)
75	2850	≤3	12.4	0.7
53	2360	≤7	16.5	5.2

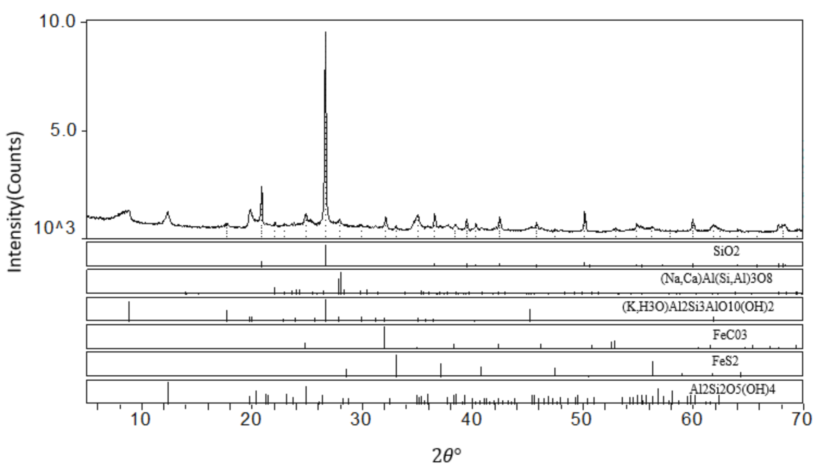

Figure 2. Gangue XRD test results.

Table 4. Main chemical composition and content of coal gangue /%.

Element	Content (%)
Montmorillonite	-
quartz	41
Potash feldspar	-
Plagioclase	4
Siderite	4
Kaolinite	17
Illite	30
Pyrite	2
other	2

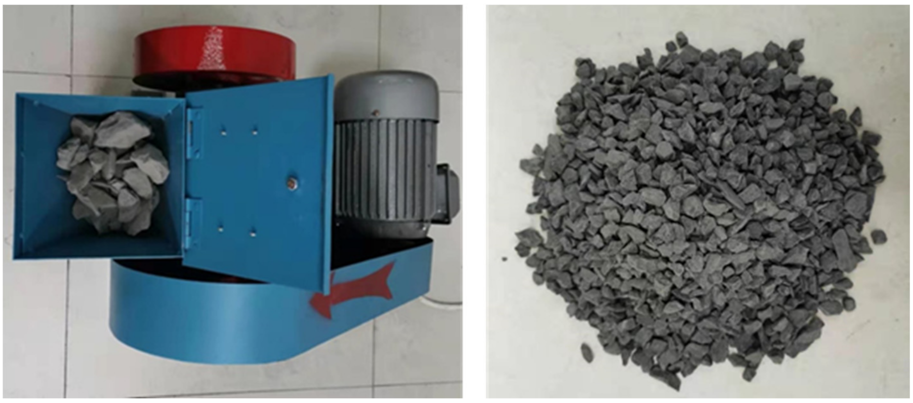

Figure 3. Crushing and screening of gangue.

2.2. Specimen Preparation

This paper focuses on the effect of gangue-, fly-ash-, polycarboxylate-superplasticizer- and steel-fiber-admixture rate on the slump expansion, 28 d mechanical properties and abrasion resistance of concrete, and it also tries to determine the optimum mix ratio. Most scholars [10,27,28] set the range of fly-ash dosing between 10–40% of the amount of cementitious material, polycarboxylate superplasticizer between 0.5–1.5% of the amount of cementitious material, and steel-fiber dosing less than 2% of the weight of concrete. There is no specific range for setting the amount of gangue, but its performance is better under the conditions of less than 40% of the weight of coarse aggregate. This study is based on other scholars' studies and determined more accurate optimal dosing ranges for each factor, especially the optimal dosing rate of gangue. It set the amount of the fly-ash admixture in the cementitious material at 20%, 25% and 30%, the amount of gangue admixture in the total amount of coarse aggregate at 20%, 30% and 40%, the amount of polycarboxylate-superplasticizer admixture in the powder material at 0.5%, 1% and 1.5%, and the amount of steel-fiber admixture at 0.5%, 1% and 1.5% of the total weight of concrete. According to the standards GB/T50080-2016 Standard for Test Method of Performance on Ordinary Fresh Concrete [29] and 283-2012 Technical Regulations for the Application of Self-compacting Concrete [30], a four-factor, three-level orthogonal experimental design was developed using the orthogonal experimental method. Mark the levels of each factor as K1, K2 and K3, and the mean value of each factor levels as $\overline{k_1}$, $\overline{k_2}$ and $\overline{k_3}$. The range result is marked as R and the standard deviation result is marked as σ. In order to facilitate the comparative effect analysis, a group of ordinary concretes without gangue, fly ash, polycarboxylate superplasticizer and steel fiber was designed as the control group. The experiment was carried out in strict accordance with the protocol, with a concrete design strength of C30 and a design fluidity class of SF2, 660 mm–750 mm.

In this experiment, the polycarboxylate-superplasticizer type with a water-reduction rate of 25% was used, and the experimental formulation was precisely calculated as shown in Table 5.

Table 5. Experimental scheme (unit: kg /m^3).

Factors	Water	Cement	Fly Ash	Fine Aggregeat	Gravel	Gangue	Superplasticizer	Steel Fiber
1	181	352	88	754	704	176	2.20	11.5
2	178	335	112	754	704	176	4.47	23
3	175	315	135	754	704	176	6.75	34.5
4	181	352	88	754	616	264	4.40	34.5
5	178	335	112	754	616	264	6.71	11.5
6	175	315	135	754	616	264	2.25	23.0
7	181	352	88	754	528	352	6.60	23.0
8	178	335	112	754	528	352	2.20	34.5
9	175	315	135	754	528	352	4.50	11.5
10	200	445	0	754	880	0	0	0

The molds were standard iron triplex molds (100 mm × 100 mm × 100 mm) and the concretes were cured for 28 d under standard concrete-making and curing protocols. Figure 4 shows some of the experimental raw materials and curing of the concrete.

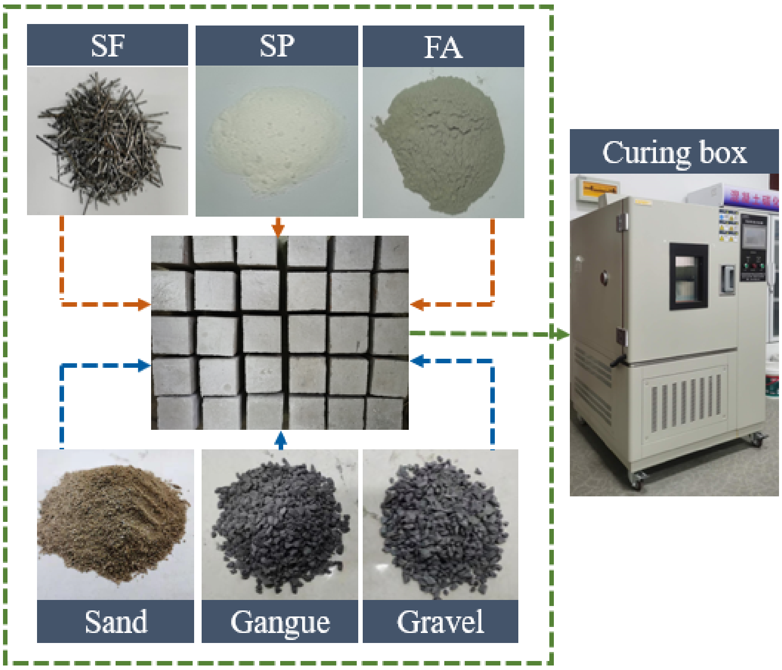

Figure 4. Experimental materials and maintenance.

2.3. *Testing Method*

2.3.1. Industrial Analysis of Coarse Aggregate

The gangue and limestone were washed and dried, then they were ground into powder using a grinding dish and screened by a circular sieve with a diameter of 0.3 mm. After screening the powders were weighed and dried; the temperature was set to 80 °C and the powder was taken out to be weighed every 1h until the weight was constant. The indicators of moisture and volatile content in gangue and limestone were determined using WS-G818 automatic industrial analyzer. The experiments were carried out with reference to the standard GB/T212-2008 "Proximate analysis of coal" [31].

The experiment was carried out by adding gangue powder and limestone powder to the crucible with a sampling spoon, and the temperature of the industrial analyzer was set to 105 °C, 815 °C and 900 °C. When the crucible temperature rose from room temperature to 105 °C, the reduction in the weight of the powder in the crucible was the moisture content in gangue powder and limestone powder. As the crucible temperature gradually increased to 815 °C, the change in the weight of the crucible was used to determine the ash component in gangue and limestone. As the crucible temperature gradually increased to 900 °C, the change in the weight of the crucible was used to determine the volatile component in gangue and limestone.

2.3.2. Slump-Expansion Test

The first nine groups were proportioned according to the experimental protocol in Table 5 and mixed using a mixer according to the standard experimental method. Since the control group had no slump-expansion phenomenon, its slump expansion could not be measured, so no slump-expansion experiment was conducted. The experiment was carried out according to GB/T50080-2016 Standard for Test Method of Performance on Ordinary Fresh Concrete [29]. Figure 5 shows the slump-expansion effect on experimental group 6. It can be seen from Figure 5 that no water secretion occurred after the concrete slumped.

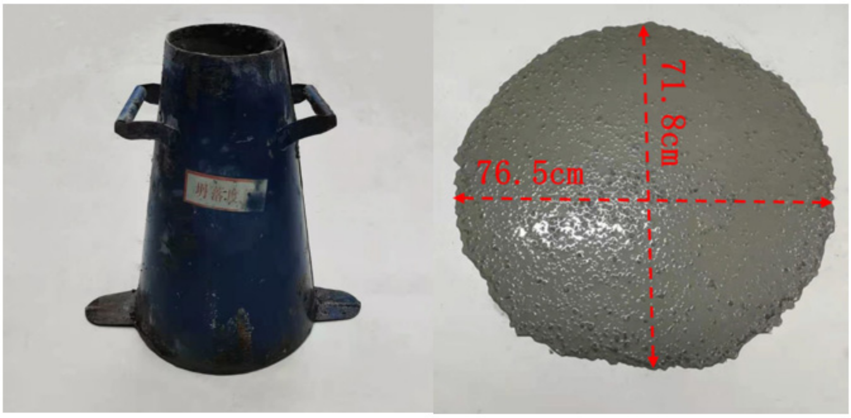

Figure 5. Slump expansion of concrete.

2.3.3. Mechanical-Property Experiment

After the concrete specimens had been cured for 28 d, concrete-compression tests and concrete-splitting tests were carried out. The experiments were carried out under the SHIMADZU AGX-250 pressure-testing machine. To minimize experimental errors, three pieces of concrete made from the same batch were used for each set of experiments and the strength was taken from their average value. The standard in GB/T 50081-2002 “Standard for test method of mechanical properties on ordinary concrete” was strictly followed [32].

2.3.4. Abrasion-Resistance Test

The concrete test block was clamped and a line was drawn in the middle of the concrete surface to mark the position to be worn. The angle grinder handle was fixed in position and a 4 mm-thick grinding wheel was used for the concrete-abrasion test. During the abrasion test, the angle grinder was placed at the position to be worn and the test was carried out by its own weight without any artificial force being applied. One concrete specimen (100 mm × 100 mm × 100 mm) was used for each group of tests. The testing time was controlled at 30 s and the angle grinder at a speed of 11,000 r/min, as shown in Figure 6. To ensure the reliability of the experiment, abrasion-resistance tests were carried out on all six faces of each specimen and the length (L) and depth (H) of the abrasion marks were recorded and their average values were taken as the test results, respectively. The L × H × 4 mm (wheel thickness) was used to approximate the concrete wear volume. As the same grinding wheel was used for this experiment, the thickness of the wheel could be ignored and L × H was taken to approximate the degree of concrete wear damage. The higher the value, the lower the abrasion resistance of the concrete.

2.3.5. Experiment of ITZ Structure Observation

To better characterize the ITZ (interfacial transition zone) between aggregate and cement mortar and to ensure an effective combination of them, this study innovatively introduced the slurry-encapsulated-aggregate experiment, which made microscopic experiments such as SEM and EDS more convenient to be carried out, and could better combine with macroscopic mechanical properties to improve the reliability of the results.

Relatively flat pieces of gangue and limestone were selected, and their surfaces were rinsed with water to remove impurities, and then one side was smoothed out followed by drying in a vacuum-drying oven for 30 min at a set temperature of 100 °C. After finishing drying, the material was taken out and cooled to room temperature in a room environment. The slurry material was prepared according to the experimental proportions shown in Table 6.

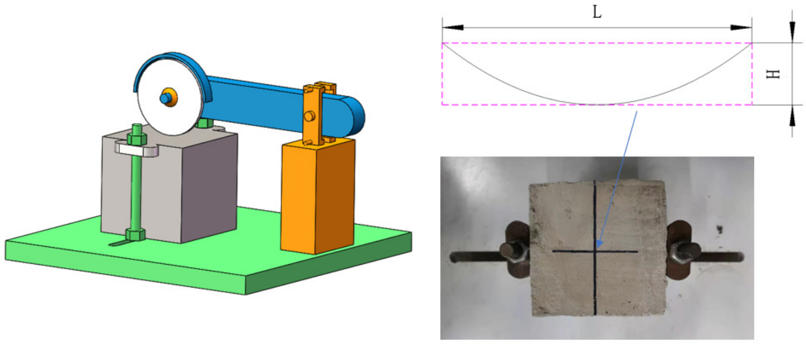

Figure 6. Abrasion-resistance test of concrete after 28 d.

Table 6. Paste proportion table.

	Group	Cement/g	Fly Ash/g	Superplasticizer/g
Gangue formation	1	100	0	0
	2	70	30	0
	3	70	30	1
Gravel formation	4	100	0	0
	5	70	30	0
	6	70	30	1

The smoothed surfaces of the gangue and limestone were plastered and maintained in a maintenance box at a temperature of 20 ± 2 °C and a humidity of 95% for 7 d. They were then broken up in order to collect aggregates with edge lengths/diameters of about 10 mm and thicknesses of 2 mm to 3 mm. The aggregate-slurry surface thickness was controlled to within 0.1 mm for scanning-electron-microscopy (SEM) analysis and X-ray energy-dispersive spectrometer (EDS). Figure 7 shows plastering experimental drawings of Groups 1–6.

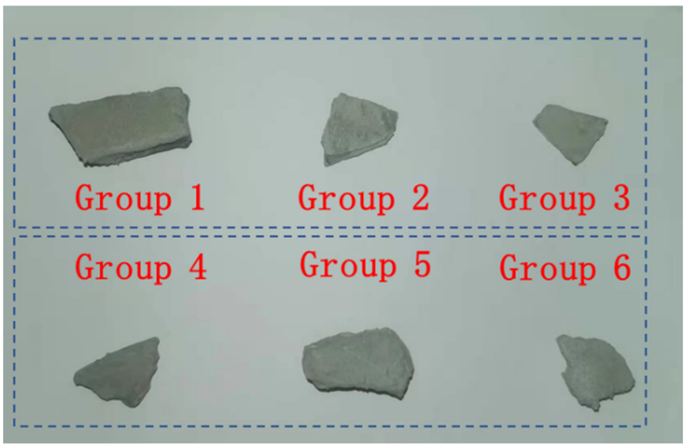

Figure 7. Plastering experiment.

3. Results and Discussion

The results of the industrial analysis of the aggregates are summarized in Table 7 and the experimental results of slump expansion, compressive strength, splitting resistance and abrasion resistance are summarized in Table 8. Range analysis and standard-deviation analysis were conducted for each factor, and the results are shown in Table 9 and Figure 8.

Table 7. Aggregate industry analysis.

	Moisture Content %	Volatile Content %	Ash Content %	Fixed Carbon Content %
Gangue	0.57	8.63	90.80	3.59
Gravel	0.41	1.58	98.01	0

Table 8. Experimental results.

Groups	Slump Flow/mm	Compressive Strength/MPa	Splitting Strength/MPa	Wear Mark		
				L/mm	H/mm	L × H/mm^2
1	706	28.14	4.02	25	4.1	102.5
2	731	28.73	4.98	22	2.9	63.8
3	750	27.73	4.55	21	2.2	46.2
4	714	31.74	6.47	25	3.9	97.5
5	740	32.12	5.09	30	5.0	150
6	741	35.87	7.25	24	3.1	74.4
7	729	28.81	5.19	35	5.5	192.5
8	723	29.25	5.42	33	5.0	165
9	747	30.27	5.55	37	6.1	225.7
10	/	33.58	5.26	23	3.3	75.9

Table 9. Range and standard deviation analysis.

Factors		Slump Flow/mm	Compressive Strength/MPa	Splitting Strength/MPa	Wear Mark (L × H/mm^2)
Fly ash	$\overline{k_1}$	716	29.56	5.23	130.83
	$\overline{k_2}$	731	30.03	5.16	126.27
	$\overline{k_3}$	746	31.29	5.78	115.43
	R	30	1.73	0.62	15.40
	σ	25.69	1.55	0.59	13.70
Gangue	$\overline{k_1}$	729	28.20	4.52	70.83
	$\overline{k_2}$	732	33.24	6.27	107.30
	$\overline{k_3}$	733	29.44	5.39	194.23
	R	4	5.04	1.75	123.40
	σ	3.53	4.55	1.52	109.97
Superplasticizer	$\overline{k_1}$	723	31.09	5.56	113.97
	$\overline{k_2}$	731	30.25	5.67	129.00
	$\overline{k_3}$	740	29.55	4.94	129.57
	R	17	1.54	0.73	15.60
	σ	14.17	1.33	0.68	15.33
Steel fiber	$\overline{k_1}$	731	30.18	4.89	159.40
	$\overline{k_2}$	734	31.14	5.81	110.23
	$\overline{k_3}$	729	29.57	5.48	102.90
	R	5	1.57	0.92	56.5
	σ	4.06	1.36	0.81	53.21

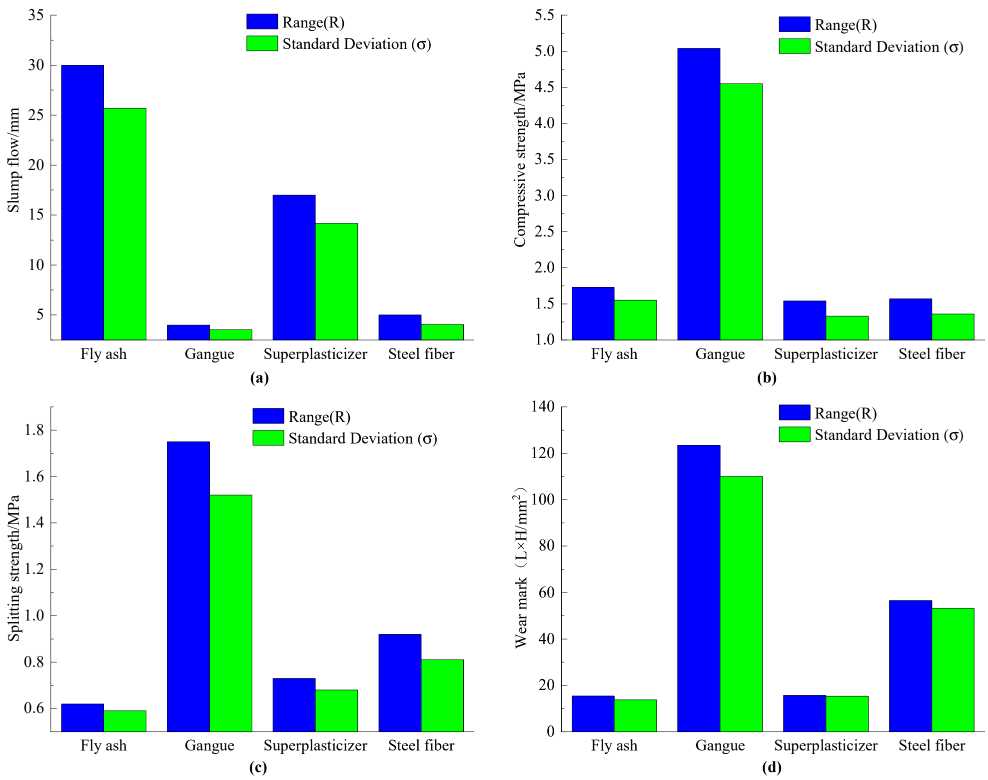

Figure 8. Range and standard-deviation results. (**a**) The influence of various factors on the slump flow of concrete. (**b**) The influence of various factors on the compressive strength of concrete. (**c**) The influence of various factors on the splitting strength of concrete. (**d**) The influence of various factors on the wear resistance of concrete.

Figure 8 shows the range and standard-deviation results of the designed experiment. It can be seen from Figure 8a that fly ash and polycarboxylate superplasticizer had a great impact on the slump expansion of SCC designed in this paper. It can be seen from Figure 8b that gangue had the greatest influence on the compressive strength of SCC. Figure 8c shows that the main factor affecting the splitting strength of SCC was still the influence of gangue, and the influence of steel fibers on the splitting strength of SCC increased. In Figure 8d, the main factors affecting the abrasion resistance of SCC were gangue and steel fibers. Therefore, when obtaining the optimal ratio of SCC, we should pay attention to the effect of fly ash and polycarboxylate superplasticizer on slump expansion, as well as the influence of gangue and steel fiber on compressive strength, splitting strength and abrasion resistance.

3.1. Aggregate Industry Analysis

According to experimental results in Table 7, it can be seen that the difference between gangue and ordinary limestone mainly lies in their content of volatile components, and that gangue's structure is less stable than that of limestone. At 900 °C the gangue's structure changes more obviously, from the original crystalline phase to amorphous SiO_2 and Al_2O_3 and metakaolinite [33]. However, the composition of limestone is mainly $CaCO_3$, which is not easy to decompose at 900 °C and it usually needs to reach the temperature of 1000–1300 °C before it can decompose into quicklime (CaO) and release CO_2 [34]. In addition, according to Table 7, it can also be seen that the bound water in gangue was 39% higher than in limestone.

3.2. Slump Flow

It can be seen from Table 8 and Figure 8a that in the concrete slump-expansion test, the designed experimental groups met the design expansion requirements, and the main factors affecting the concrete expansion were the content of fly ash and polycarboxylate superplasticizer. Within a certain range, the slump expansion of concrete was positively correlated with the content of fly ash, as shown in Figure 9a. The reasons for this are mainly (1) fly-ash morphology is mostly spherical; when it is mixed into the concrete, the frictional resistance between cement particles, or between cement particles and aggregates is reduced, making the concrete flow more easily; (2) The volume of fly ash in the slurry rises and the volume of cement in the slurry falls. Cement mixed with water becomes a viscous, non-Newtonian fluid, and the incorporation of appropriate fly ash reduces the viscosity of the slurry and increases the flow capacity [18]. In a certain range, the relationship between polycarboxylate-superplasticizer dosing and the concrete slump expansion also showed a positive rising trend, as shown in Figure 9c. The addition of polycarboxylate superplasticizer can make cement particles have the same kind of charge. According to the principle of mutual repulsion of homogeneous charges, the repulsive force between cement particles increases and free water will be released from the wrapped cement, resulting in an increase in the concrete's flow ability [35].

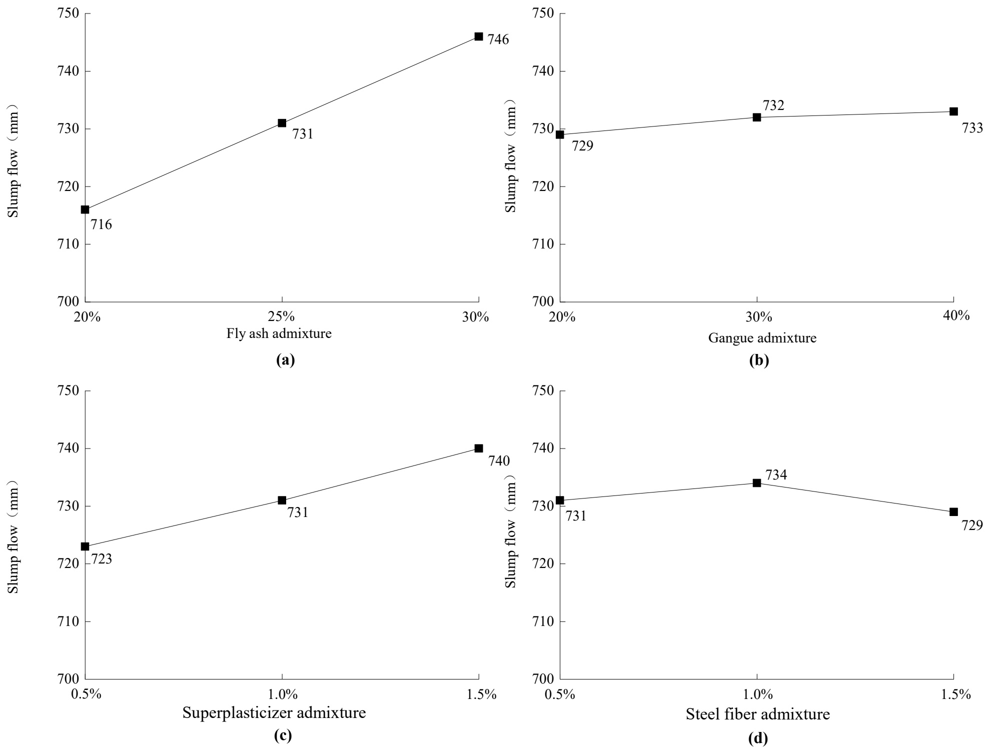

Figure 9. Influence of various factors on slump flow of concrete. (**a**) The influence of fly ash on the slump flow of concrete. (**b**) The influence of gangue on the slump flow of concrete. (**c**) The influence of superplasticizer on the slump flow of concrete. (**d**) The influence of steel fiber on the slump flow of concrete.

The influence of gangue and steel fiber on the slump expansion of concrete was relatively weak. With the increase in gangue content, the slump expansion had no obvious change trend, as shown in Figure 9b. When steel fiber's mass accounted for less than or equal to 1% of the concrete volume weight, there was no obvious influence on the slump expansion of concrete. When the mass of steel fiber was greater than 1% of the concrete volume weight, the long strip of steel fiber played a certain obstructive effect on the slump expansion of concrete, and the curve showed a decreasing trend, as shown in Figure 9d. If the amount of steel fibers continues to increase, the hindering effect becomes more obvious, and the slope of the curve decreases even more.

3.3. Compressive Strength

It can be seen from Figure 10 that under the synergistic action of fly ash, gangue, polycarboxylate superplasticizer and steel fiber, the compressive strength of concrete decreased compared with the control group, but this decrease does not include the optimized proportioning scheme, but only represents the influence of various factors on the compressive strength of concrete. According to the results in Figure 8b, the gangue greatly affected the compressive strength of concrete. Because the strength of gangue was lower than that of limestone, the overall strength of concrete decreased.

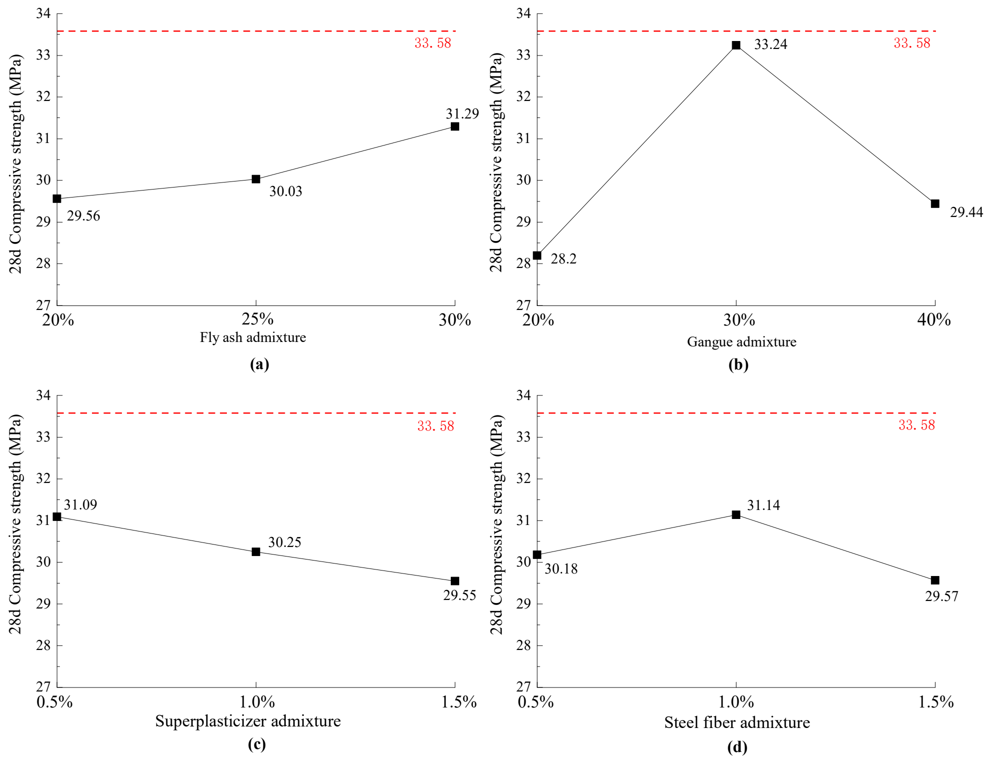

Figure 10. Influence of various factors on compressive strength of concrete. (**a**) The influence of fly ash on the compressive strength of concrete. (**b**) The influence of gangue on the compressive strength of concrete. (**c**) The influence of superplasticizer on the compressive strength of concrete. (**d**) The influence of steel fiber on the compressive strength of concrete.

In a certain range (20–30%), with the increase in dosage of fly ash, the compressive strength of concrete showed an upward trend, as shown in Figure 10a. The reasons for this may be (1) with the increase in the amount of fly ash, the amount of cement is reduced, the degree of the exothermic cement-hydration reaction is reduced, the temperature difference between the internal and external surfaces of the concrete is reduced, thus the number of temperature cracks is reduced, and the internal stress in the concrete is reduced. (2) The spherical form of fly ash reduces friction and fills in between the aggregate and the cement, thus improving the compactness of the concrete. (3) The "volcanic ash effect" of fly ash is stimulated. It reacts with cement-hydration products $Ca(OH)_2$ to produce hydrated calcium silicate and hydrated calcium aluminate crystals whose structures are more stable, resulting in an increase in the compressive strength [36].

Within a certain range (20–40%), the compressive strength increased and then decreased with the constant increase in gangue, as shown in Figure 10b. When the gangue replacement rate increased from 20% to 30%, the compressive strength of concrete rose, which may be due to reasons such as the reduction in the pores and bubbles in the interface transition zone (ITZ), thus the strength of ITZ increased.

Related studies have shown [37] that concrete is divided into Coarse Aggregate (CA), Cement Mortar (CM) and ITZ, as shown in Figure 11a. In general, the CA is the strongest zone in concrete, followed by the CM, and the ITZ zone is the weakest as it contains more harmful pores and air bubbles than CA and CM. When the concrete is under pressure, cracks spread relatively easily from the ITZ and have the most difficulty passing through the aggregate. Therefore, the initial crack has a higher probability of spreading along the ITZ until they reach the CM. As the pressure continues to rise, the number of cracks will gradually increase and become longer, interconnecting to form a spatial network, causing the concrete to fail and break down, as shown in Figure 11b.

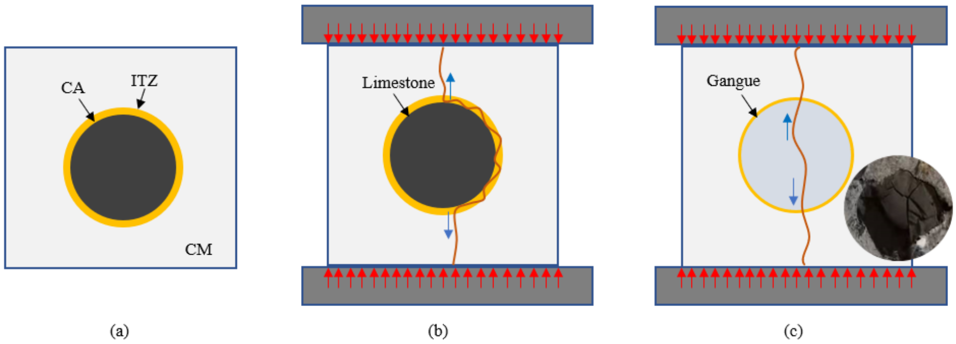

Figure 11. Relationship between aggregate type/crack path and ITZ. (**a**) The relationship between Coarse Aggregate, Cement Mortar and ITZ. (**b**) Crack propagation path in limestone concrete. (**c**) Crack propagation path in gangue concrete.

Related studies have shown that the ITZ (gangue) is thinner and denser than other types of ITZ (aggregate), so that the ITZ (gangue) has fewer cracks, pores and bubbles, which makes a higher ITZ (gangue) strength than ITZ (limestone) strength [8]. As CA (gangue) strength is lower than that of CA (limestone), when concrete is subjected to compressive stresses, the gangue's internal structure is firstly destroyed, the probability of cracks generated from internal gangue increases, then the cracks spread to the ITZ, and then to the CM, so crack expansion may occur in a shortened path, resulting in a reduction in the energy absorption of the concrete to reach breaking conditions as well as a reduction in the strength of the concrete, as shown in Figure 11c.

To further verify this conclusion, ITZ-observation experiments for gangue and limestone were designed, and the experimental method has been previously described. Group 3 and Group 6 can reflect the interfacial characteristics of the slurry material and coarse aggregate under the condition of the joint effort of fly ash and polycarboxylic acid high-efficiency water-reducing agent, thus they are taken as the representatives for the study. The results of their SEM experiments are shown in Figures 12 and 13. Figure 12 shows the results of the ITZ (gangue) scan and Figure 13 shows the results of the ITZ (limestone) scan. A comparison of the two figures shows that ITZ (gangue) produced an abundant number of needle and rod AFT crystals, while ITZ (limestone) was observed to have a predominance of fibrous, flocculent C-S-H gels, accompanied by a small number of $Ca(OH)_2$ crystals with AFT crystals. Related studies have shown that the presence of AFT and AFM crystals favors the development of the initial strength of concrete [37], resulting in higher ITZ (gangue) strength than ITZ (limestone) strength. As one of the main hydration products of cement, C-S-H contributes to the improvement of ITZ strength, but it can be clearly observed from the Figure 13 that C-S-H in ITZ (limestone) is dominated by flocculent structure, the ITZ has larger pores, and it does not contribute much to strength development. The C-S-H structure can be effectively improved and the ITZ strength can be improved by adding micro-silica fume, and by other means [21].

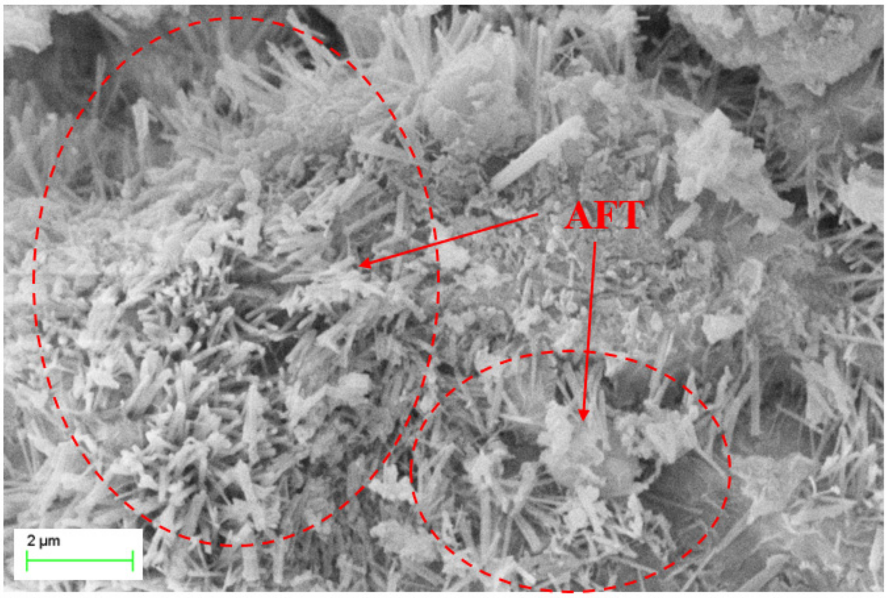

(**a**)

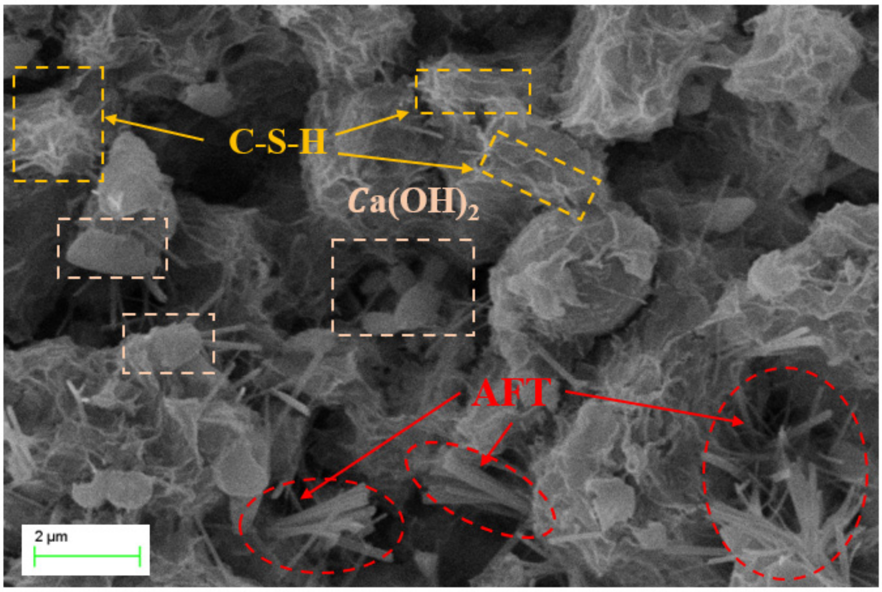

(**b**)

Figure 12. ITZ (gangue) SEM experimental results (Group 3). (**a**) ITZ (gangue) scan results 1. (**b**) ITZ (gangue) scan results 2.

X-ray energy spectra were recorded for Group 3 and Group 6 in Table 6. The experimental results are shown in Table 10 and Figure 14.

Table 10. Quality of main elements (%).

Quality	O	Ca	C	Si	Al
Group 3	42.41	25.02	11.92	9.27	6.11
Group 6	44.03	28.57	12.81	6.58	2.60

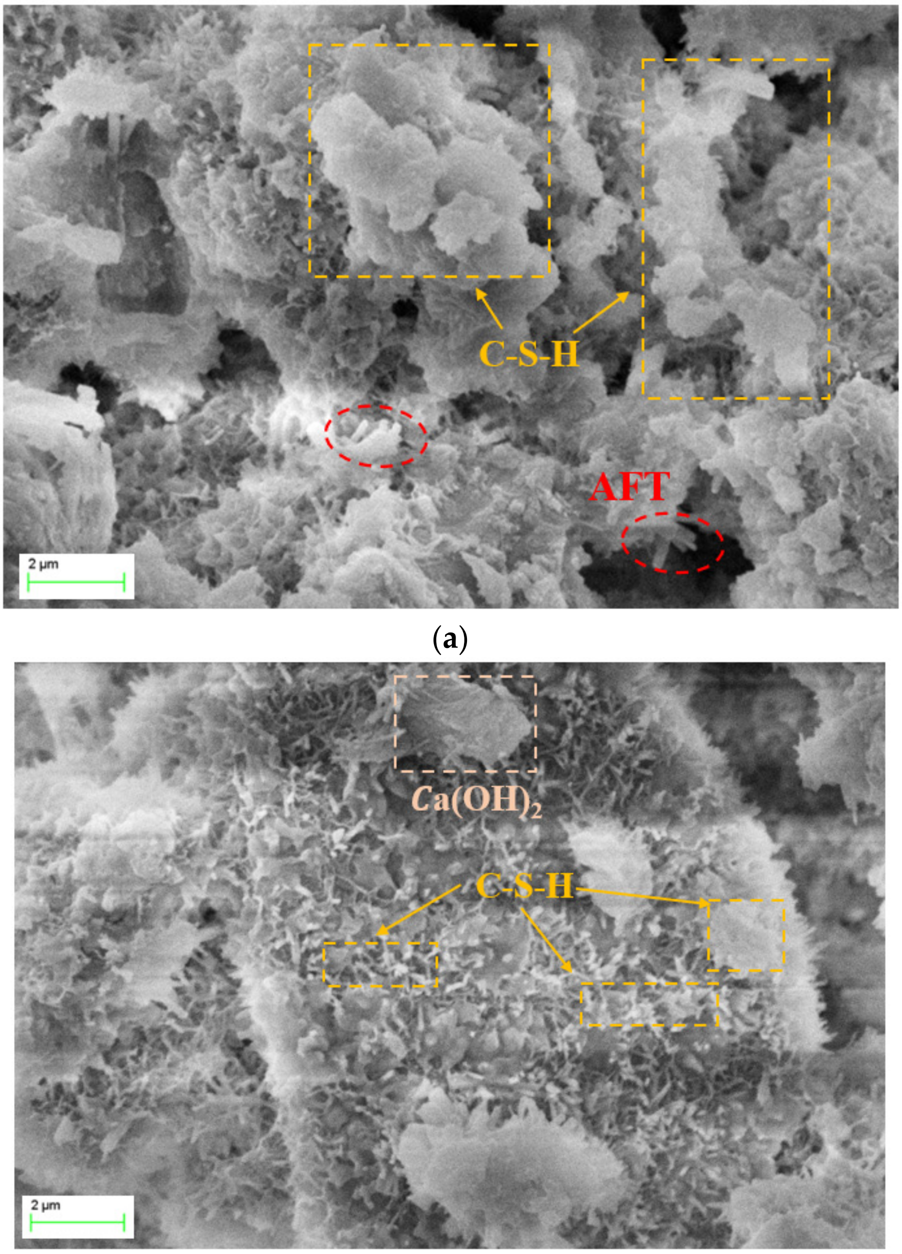

(**a**)

(**b**)

Figure 13. ITZ (limestone) SEM results (Group 6). (**a**) ITZ (limestone) scan result 1. (**b**) ITZ (limestone) scan result 2.

In Table 10, it can be seen that the content of elemental Si in Group 3 is 9.27% and that of elemental Al is 6.11%. The content of these two elements in Group 6 is 6.58% and 2.60%, respectively. The elemental Si and Al in Group 3 are 40.88% and 135% higher than that in Group 6, respectively. In Figure 14, the elemental Si and Al in Group 3 also show higher cps (count per second, representing their content) values than Group 6. Combining the results in Table 4 and Figure 2, the reason for this phenomenon may be that the gangue, with 41% quartz, 30% illite and 17% kaolinite as the main components, is rich in Si and Al, and Al is one of the main elements involved in the reaction to produce AFT and AFM crystals. The hydration products of cement react with water in the presence of gypsum $CaSO_4$ to form AFT rod crystals, which are partially transformed into AFM crystals. The reaction equation is shown in Figure 15.

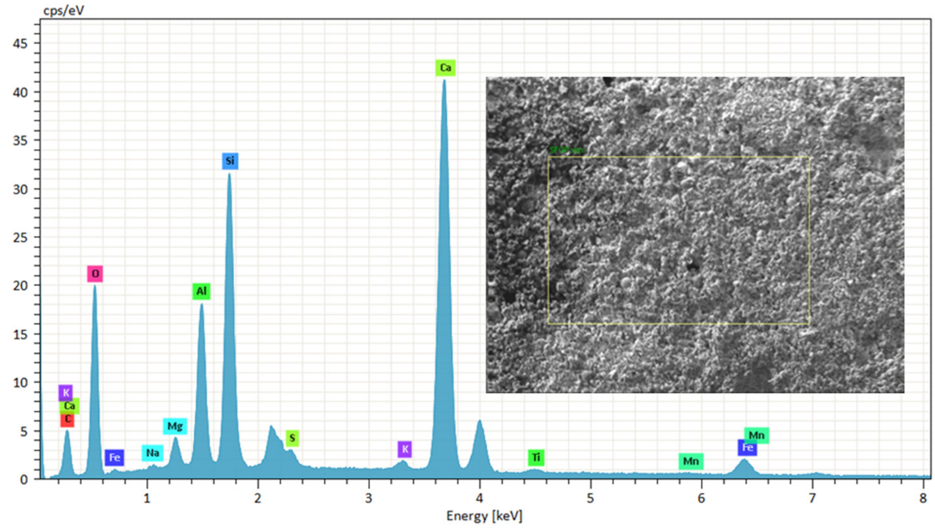

(**a**)

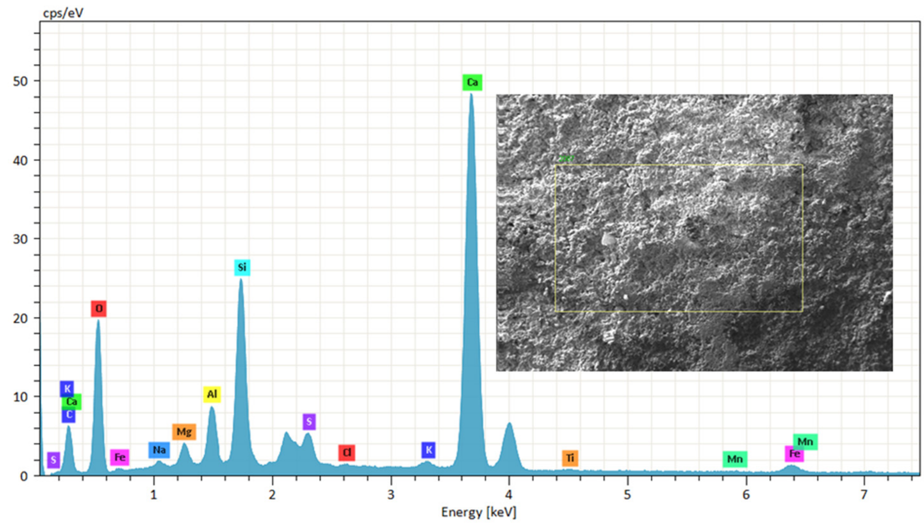

(**b**)

Figure 14. X-ray energy-spectrum analysis. (**a**) Group 3 experimental results of X-ray energy-spectrum analysis. (**b**) Group 6 experimental results of X-ray energy-spectrum analysis.

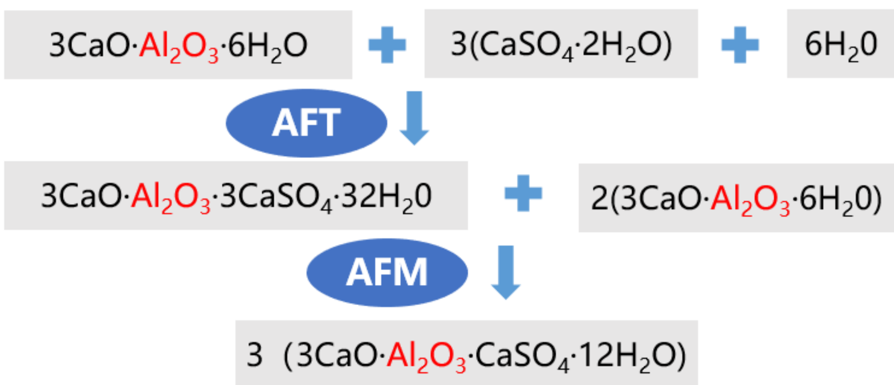

Figure 15. Reaction formula of AFT and AFM.

The hydration reaction of cement gives off a large amount of heat, which in Group 3 created the necessary temperature conditions for the generation of AFT and AFM crystals, resulting in more rod-shaped crystals of AFT and AFM being generated in Group 3 of the gangue group than in Group 6 of the limestone group.

Therefore, under the conditions that the aggregate particle size ranged from 5 mm to 15 mm and gangue was present in an amount of about 30%, the development of concrete strength was better. When the gangue admixture rate was more than 30%, due to the strength of gangue being less than that of limestone, the skeleton strength weakened more obviously, resulting in the reduction of compressive strength of concrete. It may be feasible to use various research methods such as improving the gangue temperature or increasing its specific surface area in order to further stimulate the gangue surface activity, improve the strength of the transition zone at the interface between gangue and slurry, and then improve the ability of concrete to accommodate the gangue, but the gangue processing costs will also be increased, so it still needs to be further studied by scholars.

Under the conditions of a certain water–cement ratio, with the increase in dosage of the polycarboxylate superplasticizer, the compressive strength of concrete showed a decreasing trend, as shown in Figure 10c. The reasons for this may be: (1) under the conditions of a certain water–cement ratio, the increase in the amount of polycarboxylate superplasticizer is equivalent to an increase in the water–cement ratio of the concrete, the liquidity of the cement mortar increases and its bonding capacity decreases, the bonding capacity with the aggregates and fibers also decreases, and the strength of the concrete-cement-mortar layer decreases, resulting in a decrease in the strength of the concrete. (2) Although polycarboxylate superplasticizer improves the workability of concrete when mixed with cement mortar, it also produces a certain amount of air bubbles into the concrete as it reacts with water [35]. If the cement does not add any water-reducing agent, CaO, Al_2O_3 and other elements will have hydration reactions, attracting water molecules in the vicinity of cement particles, which will flocculate and bond together, as shown in Figure 16a; when the appropriate amount of polycarboxylate superplasticizer is added, the water-reducing-agent particles cause the cement particles to have the same electric charge, which in turn causes the cement particles to disperse due to electrostatic repulsion, and the agglomeration phenomenon is obviously reduced. The concrete's compatibility is improved, such as in Figure 16b; when mixed with an excessive amount of polycarboxylate superplasticizer, the amount of air bubbles also increases, reducing the compactness of the concrete, as shown in Figure 16c. Therefore, about 0.5% of the total powder material of polycarboxylate superplasticizer is the best rate for this concrete proportion.

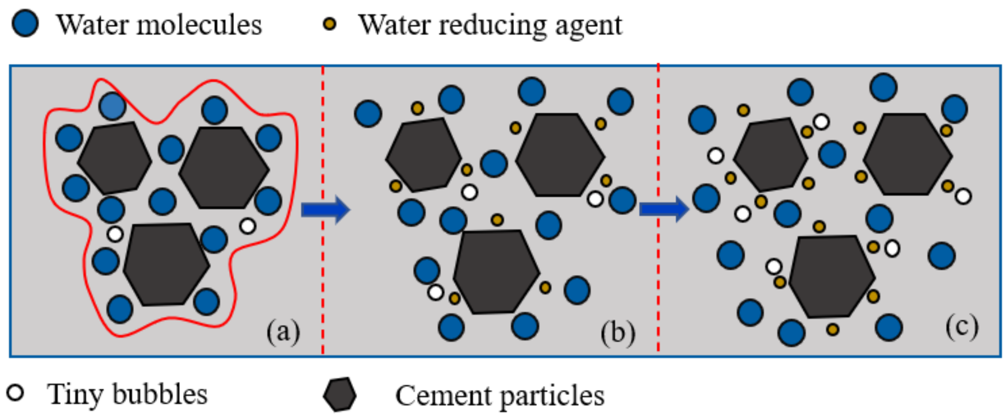

Figure 16. Strength mechanism of concrete strengthened by superplasticizer. (**a**) No superplasticizer added. (**b**) Added appropriate amount (0.5–1.0%) of superplasticizer. (**c**) Excessive (>1.0%) superplasticizer was added.

In a certain range (0.5–1.5%), with the increase in the dosage of steel fibers, the compressive strength of concrete showed a trend of initial rising and subsequent falling, as shown in Figure 10d. The reason for this may be that when concrete is under pressure, some of the pressure is transferred to the steel fibers. The concrete reaches its damage condition and an additional partial force is required to deform the fibers. When the amount of steel fibers increases to about 1.5%, the compatibility between steel fibers and coarse aggregates becomes poor, the distribution of steel fibers tends to be non-uniform when mixing, and a loose slurry interface structure tends to be produced between the grooves of the wavy steel fibers, with an increase in harmful pore bubbles. The mechanism of action of which is shown in Figure 17. In lightweight concrete, when the steel-fiber content is 1%, the compressive strength of concrete is lower [26]. Therefore, the optimal mixing ratio of steel fibers is also significantly related to the type of concrete.

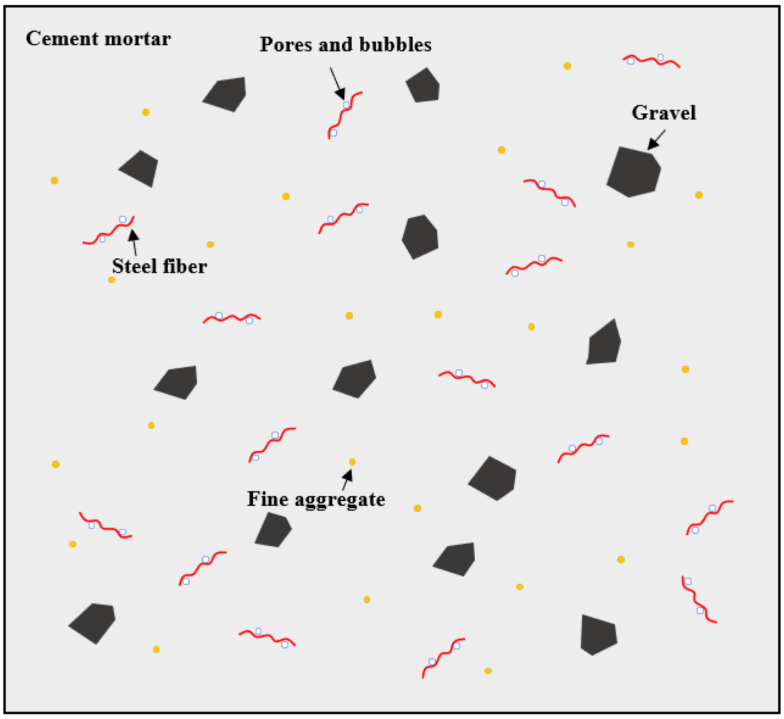

Figure 17. Internal structure of self-compacting gangue concrete.

3.4. Splitting Strength

We can see from Figure 18 that when the mixing rate of fly ash was 30%, the mixing rate of gangue was 30% and 40%, while that of polycarboxylate superplasticizer was 0.5% and 1.0%, and that of steel fiber was 1% and 1.5%, which was higher than the splitting resistance of the control group. Combined with the results in Figure 8, we can see that the influence of steel fiber on anti-splitting performance was higher than that on compressive strength, and had a better crack resistance, which made the splitting resistance of some experimental groups higher than that of the control group.

At the stage of increasing the fly-ash admixture from 20% to 25% and at the stage of increasing polycarboxylate-superplasticizer admixture from 0.5% to 1%, the splitting strength had no obvious change and was basically the same, as shown in Figure 18a,c. The splitting strength of the concrete increased at the stage of increasing the amount of fly ash to 30%, while the splitting strength of the concrete decreased when the amount of polycarboxylate superplasticizer was increased from 1% to 1.5%. The reason for this phenomenon is the same as the analysis of compressive strength in the previous section: fly ash mainly improves the slurry's compatibility and makes the concrete dense. Although the polycarboxylate superplasticizer is also beneficial to the improvement of the concrete's compatibility, under the condition of a certain water–cement ratio, excessive addition of superplasticizer will introduce harmful pores [38] and weaken the strength of cement mortar.

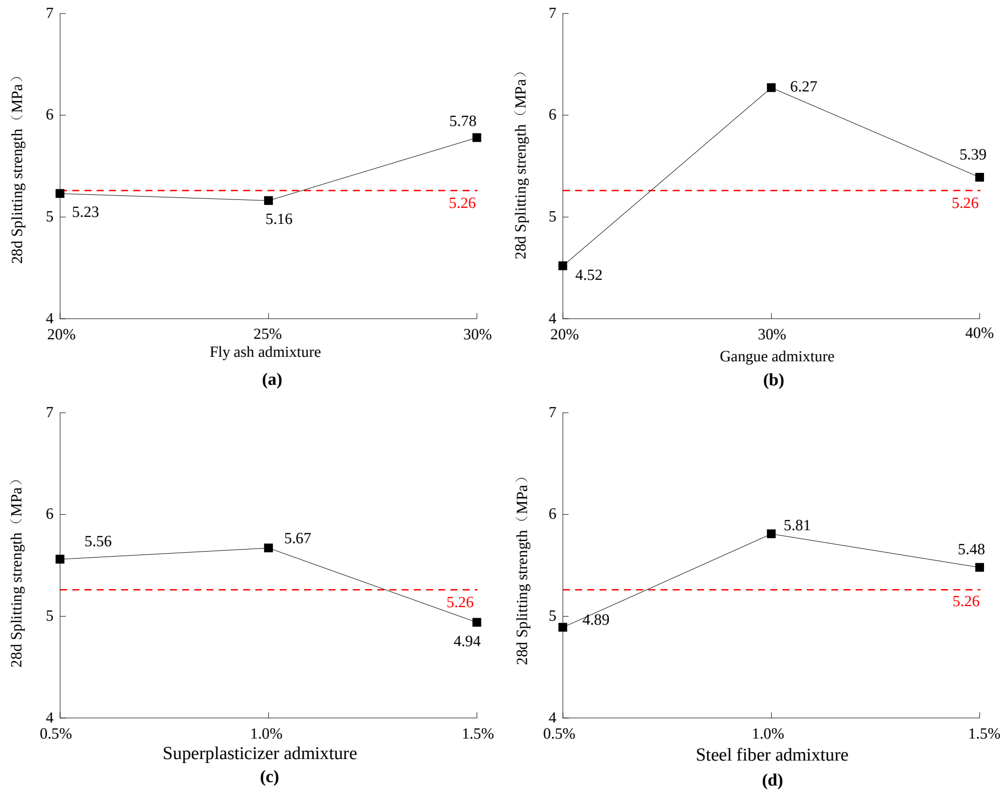

Figure 18. Influence of various factors on concrete splitting strength. (**a**) The influence of fly ash on the splitting strength of concrete. (**b**) The influence of gangue on the splitting strength of concrete. (**c**) The influence of superplasticizer on the splitting strength of concrete. (**d**) The influence of steel fiber on the splitting strength of concrete.

With the increase in the amount of admixture of gangue and steel fibers, the splitting strength firstly increased and then decreased, as shown in Figure 18b,d. According to the results in Figure 8c, gangue remains the most influential of the four factors, and the splitting-strength curve is similar to the compressive-strength curve. The gangue dosing of 30% contributed the greatest splitting resistance for the same reasons as analyzed in compressive strength, which can be explained in terms of the crack expansion path and energy consumption. The splitting resistance of the concrete was increased by about 19% at a steel-fiber admixture of 1% compared to 0.5%, while only about 3% in the compressive strength. By comparison, it was found that the improvement in the splitting resistance of the concrete by steel fibers was about six times the improvement in the compressive-strength performance. In the concrete-splitting experiments, the steel fibers mainly played a role in carrying tensile and shear stresses, and especially those in the shear region had an obvious beneficial incremental effect on the concrete's resistance to splitting. This is in agreement with the results obtained in a study by Rao [22]. This also has a similar trend to the study of Xu et al. [39], but due to the different specific proportioning schemes, the position of the curve decline is different to a certain extent.

Figure 19 reflects that the compressive strength of the concrete is essentially proportional to the splitting resistance. Of the 10 prepared groups of concrete, experiments 4–6, 9 and 10 all met the strength requirements of the preparation. In Figure 19, the closer the experiment is to the top right corner, the better the concrete performance. The analysis of Figure 19 leads to the following results: (1) In the compressive test, only in the proportioning of experiment 6, the strength of concrete was higher than that of the control experimental group 10. In the splitting-resistance experiment, experimental group 6, experimental group 4 and experimental group 9 all showed higher performance than that of the control experimental group 10, indicating that the steel fibers had a more significant improvement in the splitting strength. (2) The proportion of experiment 6 (30% of fly ash, 30% of gangue, 0.5% of high-efficiency water-reducing agent and 1% of steel fiber) was more reasonable. (3) In experiments 4–6, the compressive/splitting strength reached the design value, and it can be seen that the optimal rate of gangue should be near 30%. If the admixture is higher than 30%, then the concrete skeleton strength will be significantly reduced, resulting in deterioration of the overall mechanical properties of concrete.

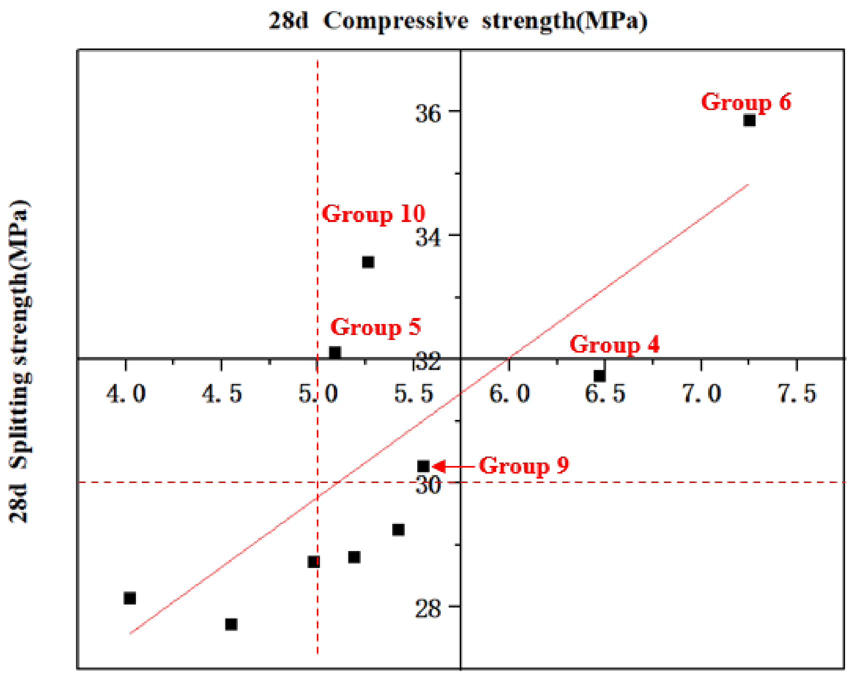

Figure 19. Axial scatter diagram of compressive strength and splitting strength.

Figure 20 shows the experimental graph of compressive/splitting damage to concrete after 28 d.

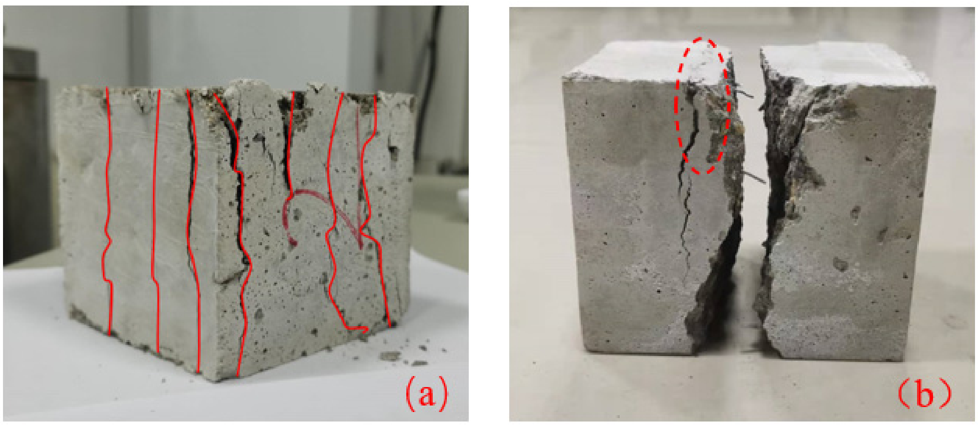

Figure 20. Compression and splitting test of concrete after 28 d (Group 2). (**a**) Group 2 concrete specimens. (**b**) Group 2 splitting damage by compression to concrete specimens.

Figure 20 reflects the damage characteristics of the concrete under the ratio set of experiment 2. Figure 20a shows the damage diagram of the concrete under compression at a strain of 5 mm, and it can be seen that after the compression, the cracks are distributed in long uniformed strips and there is still residual stress, which indicates that the steel fibers have a good crack-arresting effect. Figure 20b shows the experimental diagram of the concrete after splitting damage. It can be seen from the diagram that the presence of transversely or inclined distribution of steel fibers at the location of the splitting makes the force transferred to the concrete when the concrete is subjected to shear force, so that the force on the concrete is dispersed and cracks are produced on the left side, which further confirms that steel fibers have a better crack-arresting effect under tensile stress.

3.5. Experimental Results of Abrasion Resistance

As can be seen from Figure 21, under the synergistic action of four factors, only when the ratio of gangue is 20%, the wear amount is slightly lower than that of the control group. According to the results in Figure 8d, the main factors affecting the abrasion resistance of concrete are gangue and steel fiber, and the gangue has the greatest negative impact, resulting in the overall abrasion resistance of concrete being lower than that of the control group.

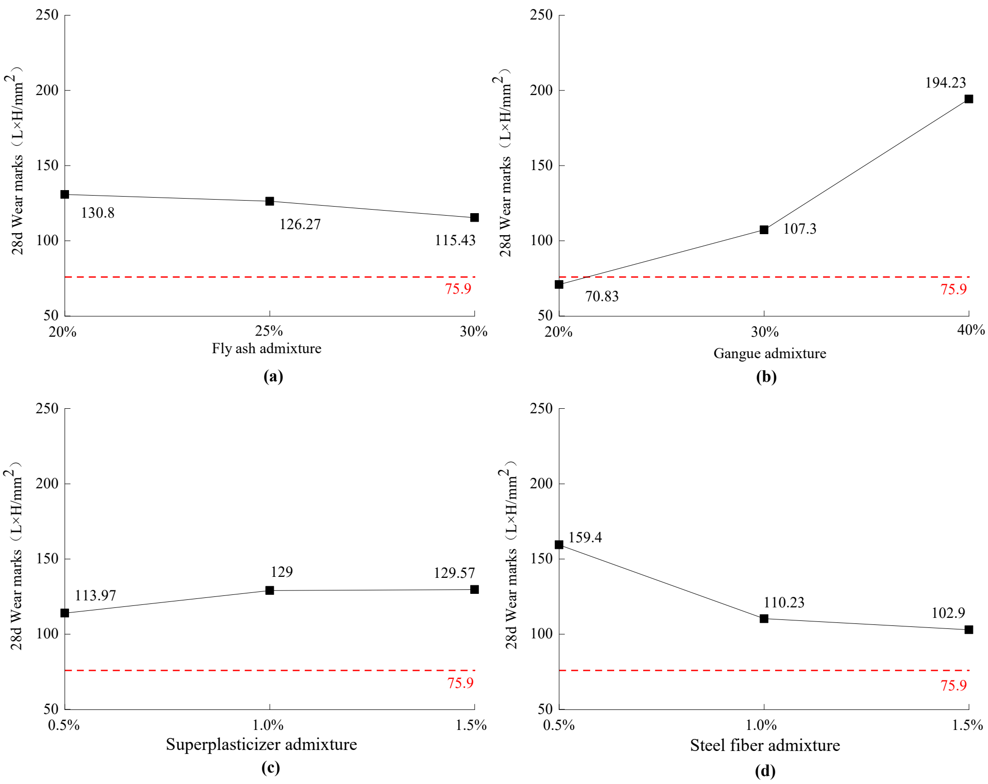

Figure 21. Influence of various factors on abrasion resistance of concrete. (**a**) The influence of fly ash on the wear resistance of concrete. (**b**) The influence of gangue on the wear resistance of concrete. (**c**) The influence of superplasticizer on the wear resistance of concrete. (**d**) The influence of steel fiber on the wear resistance of concrete.

A small increase can also be seen in the abrasion resistance of concrete with the increase in the amount of fly ash, as shown in Figure 21a. Because with the increase in the amount of fly ash, the small pores in the concrete are gradually filled and the overall structural compactness is enhanced, which enhances the abrasion resistance of the concrete.

With the increase in the amount of gangue, the concrete abrasion resistance decreased, abrasion increases at a greater rate in the 30–40% admixture than in the 20–30% admixture, and this result is to be expected, as shown in Figure 21b. As the gangue's own strength is relatively low, and its abrasion resistance is lower than that of ordinary limestone. When added in concrete, the wea, thinning and fractures of the gangue are unavoidable. However, at 30% admixture, the reduction in abrasion resistance of the concrete is still within acceptable limits.

Under certain conditions of water–cement ratio, the abrasion resistance of concrete decreases with the increase in polycarboxylate superplasticizer, which is caused by the increase in polycarboxylate-superplasticizer dosage leading to the decrease in cement-mortar strength and weakening of bonding force, making the cement-mortar layer of concrete easier to be peeled off, as shown in Figure 21c.

The abrasion resistance of concrete tends to increase with the increase in the number of steel fibers incorporated, as shown in Figure 21d. Due to the higher abrasion resistance of steel fibers compared to brittle aggregates and cement mortars, the incorporation of steel fibers is therefore beneficial in improving the abrasion resistance of concrete.

After the previous analysis, concrete of the experimental proportioning scheme of Group 6 showed good resistance in slump expansion, mechanical properties and abrasion resistance. Therefore, the optimum amount of gangue blending derived from this study is about 30% of the mass of coarse aggregate, the optimum amount of fly-ash blending is about 30% of the mass of cementitious material, the optimum amount of polycarboxylate-superplasticizer blending is about 0.5% of the mass of cementitious material, and the optimum amount of steel-fiber blending is about 1% of the mass of concrete material.

4. Field-Application Effect

After obtaining the optimum proportion of self-compacting gangue concrete, this study was carried out in a field trial in Lane 5315 of Shanxi Jinneng Holding Group Zhaozhuang Coal Co. The bottom thickness was 200 mm, the bottom length was 50 m, and the bottom width was 5600 mm. After the bottom was laid, watering maintenance was performed before the samples (200 mm × 200 mm × 200 mm) were taken at 7 d and 28 d, respectively, for compressive and splitting strength tests. The process is shown in Figure 22. The performance was also compared with that of conventional mine paving concrete, as shown in Table 11.

Figure 22. Field-application effect.

Table 11. Field-test intensity.

Concrete Type	Compressive Strength/MPa		Splitting Strength/MPa	
	7 d	28 d	7 d	28 d
Self-compacting gangue concrete	21.78	32.25	4.43	6.58
Traditional concrete	18.93	30.67	3.17	5.12

The compressive strengths of the concrete at 7 d and 28 d were 21.78 MPa and 32.25 MPa, respectively. Subject to the actual ambient temperature (around 10 °C) and curing conditions, the 28 d compressive strength of the concrete was lower than that derived from the experiments, but still met the requirements for use in the field.

5. Conclusions

In this paper, the optimized ratio of self-compacted gangue concrete was 30% of coarse-aggregate weight, 30% of fly-ash weight of cementitious material, 0.5% of polycarboxylate-superplasticizer weight of cementitious material, 1% of steel-fiber weight of concrete, and the relationship between ITZ microscopic properties and macroscopic mechanical properties of concrete was established.

(1) In the proportion range studied in this paper, the effect of fly ash and polycarboxylate superplasticizer on the slump expansion of SCC was higher than that of steel fiber and gangue. Concrete slump expansion was positively correlated with fly-ash- and polycarboxylate-superplasticizer-admixture rate. As steel-fiber dosage increased from 1% to 1.5%, the slump expansion of concrete exhibited an obvious downward trend, while gangue had almost no effect on the concrete slump expansion.
(2) In the proportion range studied in this paper, the effect of gangue and steel fiber on the compressive and splitting strength of self-compacting gangue concrete was higher than that of fly ash and polycarboxylate superplasticizer. With the increase in the amount of gangue and steel fibers, both the compressive and splitting strength of concrete increased first and then decreased. The optimum mixing rate was about 30% and 1%, respectively. With the increase in fly-ash dosing, both the compressive strength and the splitting strength of concrete increased and the optimum mixing rate was about 30%, respectively. With the increase in polycarboxylate-superplasticizer dosing, both the compressive strength and the splitting strength of concrete decreased and the optimum mixing rate was about 0.5%, respectively.
(3) In the proportion range studied in this paper, the effect of gangue and steel fiber on the abrasion resistance of self-compacting gangue concrete was higher than that of fly ash and polycarboxylate superplasticizer. The abrasion resistance of concrete was negatively correlated with the content of gangue and polycarboxylate superplasticizer, and positively correlated with the content of steel fiber and fly ash. The proportion of gangue significantly decreased in the range of 30–40%, but when the proportion was 30%, the concrete still had good wear resistance.
(4) Through SEM, EDS, XRD and other experiments, it was found that more AFT crystals were generated in the ITZ (gangue), while the numbers of AFT were less in the ITZ (limestone). As the gangue is mainly composed of quartz (41%), illite (30%) and kaolinite (17%), the content of Al is rich, which is conducive to the formation of AFT and AFM crystals in ITZ, which is more favorable to the development of concrete strength in the first and middle term.

Author Contributions: Formal analysis, N.G.; Project administration, L.C.; Resources, L.C. and Z.L.; Validation, G.L.; Writing—original draft, N.G., X.G. and J.Z.; Writing—review & editing, G.L. All authors have read and agreed to the published version of the manuscript.

Funding: National Natural Science Foundation of China (Grant No. 51974177, 52104206); Natural Science Foundation of Shandong (Grant No. ZR2019QEE007); Special funds for Taishan scholar project; Major scientific and technological innovation projects of Shandong Province (Grant No. 2019SDZY0203).

Institutional Review Board Statement: Not applicable.

Informed Consent Statement: Informed consent was obtained from all subjects involved in the study.

Data Availability Statement: Not applicable.

Acknowledgments: The author would like to thank all the teachers and students of the school of energy and mining engineering and the school of safety and environmental engineering of Shandong University of Science and Technology for their active participation and help in this study.

Conflicts of Interest: The authors declare no conflict of interest.

References

1. Xi, Y.; Zhang, D. Construction of "Internet + Recycling" Mode of Renewable Resources. *Res. Sci. Technol. Manag.* **2018**, *38*, 260–267.
2. Quan, Z.; Chen, Y.; Ma, R.; Liu, R. Experimental study on preparation of autoclaved aerated concrete blocks from lithium tailings sand. *New Build. Mater.* **2022**, *49*, 120–123.

3. Yang, Q.; Lü, M.; Luo, Y. Effects of surface-activated coal gangue aggregates on properties of cement-based materials. *J. Wuhan Univ. Technol.-Mater.* **2013**, *28*, 1118–1121. [CrossRef]
4. Ma, H.; Zhu, H.; Wu, C.; Chen, H.; Sun, J.; Liu, J. Study on compressive strength and durability of alkali-activated coal gangue-slag concrete and its mechanism. *Powder Technol.* **2020**, *368*, 112–124. [CrossRef]
5. Moghadam, M.J.; Ajalloeian, R.; Hajiannia, A. Preparation and application of alkali-activated materials based on waste glass and coal gangue: A review. *Constr. Build. Mater.* **2019**, *221*, 84–98. [CrossRef]
6. Ashfaq, M.; Lal, M.H.; Moghal, A.A.B.; Murthy, V.R. Carbon Footprint analysis of Coal Gangue Applications in Geotechnical Engineering. *Indian Geotech. J.* **2020**, *50*, 646–654. [CrossRef]
7. Ashfaq, M.; Heeralal, M.; Moghal, A. Utilization of Coal Gangue for Earthworks: Sustainability Perspective. 2021. Available online: https://www.researchgate.net/publication/349039269_Utilization_of_Coal_Gangue_for_Earthworks_Sustainability_Perspective (accessed on 4 February 2021).
8. Zhou, M.; Dou, Y.; Zhang, Y.; Zhang, Y.; Zhang, B. Effects of the variety and content of coal gangue coarse aggregate on the mechanical properties of concrete. *Constr. Build. Mater.* **2019**, *220*, 386–395. [CrossRef]
9. Xiao, M.; Ju, F.; He, Z.-Q. Research on shotcrete in mine using non-activated waste coal gangue aggregate. *J. Clean. Prod.* **2020**, *259*, 120810. [CrossRef]
10. Su, X. Experimental Research on Basic Mechanical Properties of Coal Gangue Concrete. *Xi'an Univ. Archit. Technol.* **2021**. [CrossRef]
11. Bai, G.; Su, Y.; Liu, H. Experimental study on the complete stress-strain curve of gangue aggregate concrete. *Ournal. Phys. Conf. Ser.* **2021**, *1904*, 012004. [CrossRef]
12. Kavitha, O.R.; Shanthi, V.M.; Prince Arulraj, G.; Sivakumar, V.R. Microstructural studies on eco-friendly and durable Self-compacting concrete blended with metakaolin. *Appl. Clay Sci.* **2016**, *124–125*, 143–149. [CrossRef]
13. Revilla-Cuesta, V.; Skaf, M.; Serrano-López, R.; Ortega-López, V. Models for compressive strength estimation through non-destructive testing of highly self-compacting concrete containing recycled concrete aggregate and slag-based binder. *Constr. Build. Mater.* **2021**, *280*, 122454. [CrossRef]
14. Choudhary, R.; Gupta, R.; Nagar, R.; Jain, A. Mechanical and abrasion resistance performance of silica fume, marble slurry powder, and fly ash amalgamated high strength self-consolidating concrete. *Constr. Build. Mater.* **2021**, *269*, 121282. [CrossRef]
15. Han, J.; Yan, P. Influence of segregation on the permeability of self-consolidating concrete. *Constr. Build. Mater.* **2021**, *269*, 121277. [CrossRef]
16. Xie, T.; Ali, M.S.M.; Elchalakani, M.; Visintin, P. Modelling fresh and hardened properties of self-compacting concrete containing supplementary cementitious materials using reactive moduli. *Constr. Build. Mater.* **2021**, *272*, 121954. [CrossRef]
17. Zhu, W.; Wei, J.; Li, F.; Zhang, T.; Chen, Y.; Hu, J.; Yu, Q. Understanding restraint effect of coarse aggregate on the drying shrinkage of self-compacting concrete. *Constr. Build. Mater.* **2016**, *114*, 458–463. [CrossRef]
18. Shi, X.X.; Liu, Y.X.; Pu, Q.; Tian, Y.; Chen, J.J. Effect of highly efficient water-reducing agent and fly ash on the performance of self-compacting concrete. *Concr. Cem. Prod.* **2017**, *12*, 14–18.
19. Qiu, J.; Zhou, Y.; Guan, X.; Zhu, M. The influence of fly ash content on ITZ microstructure of coal gangue concrete. *Constr. Build. Mater.* **2021**, *298*, 123562. [CrossRef]
20. Qiu, J.; Zhu, M.; Zhou, Y.; Guan, X. Effect and mechanism of coal gangue concrete modification by fly ash. *Constr. Build. Mater.* **2021**, *294*, 123563. [CrossRef]
21. Shcherban', E.M.; Stel'makh, S.A.; Beskopylny, A.; Mailyan, L.R.; Meskhi, B.; Varavka, V. Nanomodification of Lightweight Fiber Reinforced Concrete with Micro Silica and Its Influence on the Constructive Quality Coefficient. *Materials* **2021**, *14*, 7347. [CrossRef]
22. Rao, B.K.; Ravindra, V. Steel fiber reinforced self compacting concrete incorporating class F fly ash. *Int. J. Eng. Sci. Technol.* **2010**, *2*, 4936–4943.
23. Ghasemi, M.; Ghasemi, M.R.; Mousavi, S.R. Investigating the effects of maximum aggregate size on self-compacting steel fiber reinforced concrete fracture parameters. *Constr. Build. Mater.* **2018**, *162*, 674–682. [CrossRef]
24. Ding, X.; Zhao, M.; Zhou, S.; Fu, Y.; Li, C. Statistical Analysis and Preliminary Study on the Mix Proportion Design of Self-Compacting Steel Fiber Reinforced Concrete. *Materials* **2019**, *12*, 637. [CrossRef] [PubMed]
25. Wang, C. Analysis of the Influence of Fiber on the Working Performance and Mechanical Properties of Self-Compacting Concrete. Master's Thesis, Heilongjiang University, Harbin, China, 2021.
26. Horňáková, M.; Lehner, P. Analysis of Measured Parameters in Relation to the Amount of Fibre in Lightweight Red Ceramic Waste Aggregate Concrete. *Mathematics* **2022**, *10*, 229. [CrossRef]
27. Zhao, Q.; Xu, G.; Li, Z.; Liu, F.; He, T.; Shen, W. Research on the performance of self-compacting concrete with high-volume fly ash. *J. Wuhan Univ. Technol.* **2020**, *42*, 1–5.
28. Wang, Z.; Zhao, N. Properties of Steel Fiber Reinforced Coal Gangue Coarse Aggregate Concrete. *Wuhan Univ. J. Nat. Sci.* **2014**, *19*, 262–268. [CrossRef]
29. *GB/T 50080-2016*; Standard for Test Method of Performance on Ordinary Fresh Concrete. China Construction Industry Press: Beijing, China, 2016.
30. *JGJ/T 283-2012*; Technical Regulations for the Application of Self-Compacting Concrete. China Construction Industry Press: Beijing, China, 2012.
31. *GB/T 212-2008*; Proximate Analysis of Coal. China National Standardization Administration Committee: Beijing, China, 2008.

32. *GB/T 50081-2002*; Standard for Test Method of Mechanical Properties on Ordinary Concrete. Ministry of Construction of the People's Republic of China: Beijing, China, 2003.
33. Cao, Y.; Li, Y.; Zhang, J.; Cao, Z.; Sun, C. Effects of fineness and calcination temperature on the activity and microstructure of coal gangue pozzolan. *J. Silic.* **2017**, *45*, 1153–1158.
34. Wang, X.; Li, J.; Xue, Z. Study on the activity and grain size of calcined lime under high temperature rapid heating. *Bull. Silic.* **2016**, *35*. [CrossRef]
35. Wei, J. *Study on the Preparation and Performance of Low-Air-Entraining Polycarboxylate Superplasticizer*; Shandong University: Jinan, China, 2018.
36. Vejmelková, E.; Keppert, M.; Grzeszczyk, S.; Skalinski, B.; Cerny, R. Properties of self-compacting concrete mixtures containing metakaolin and blast furnace slag. *Constr. Build. Mater.* **2011**, *25*, 1325–1331. [CrossRef]
37. Demie, S.; Nuruddin, M.F.; Shafiq, N. Effects of micro-structure characteristics of interfacial transition zone on the compressive strength of self-compacting geopolymer concrete. *Constr. Build. Mater.* **2013**, *41*, 91–98. [CrossRef]
38. Lu, Y.; Wu, H.; Li, J.; Jiang, Y.; Li, F. Operation law of bubbles in concrete and its prevention measures. *Railw. Constr. Technol.* **2021**, *9*, 29–32+47.
39. Xu, Z.; Wu, J.; Zhao, M.; Bai, Z.; Wang, K.; Miao, J.; Tan, Z. Mechanic-al and microscopic properties of fiber-reinforced coal gangue-based geopolymer concrete. *Nanotechnol. Rev.* **2022**, *11*, 526–543. [CrossRef]